Check for updates

Structural diversity-guided optimization of carbazole derivatives as potential cytotoxic agents

Zilin Gao[1,2], Yu Chen[1], Yufei Nie[1], Keming Chen[1], Xiufang Cao[1]* and Shaoyong Ke[2]*

[1]College of Science, Huazhong Agricultural University, Wuhan, China, [2]National Biopesticide Engineering Research Centre, Hubei Biopesticide Engineering Research Centre, Hubei Academy of Agricultural Sciences, Wuhan, China

Carbazole alkaloids, as an important class of natural products, have been widely reported to have extensive biological activities. Based on our previous three-component reaction to construct carbazole scaffolds, we introduced a methylene group to provide a rotatable bond, and designed series of carbazole derivatives with structural diversity including carbazole amide, carbazole hydrazide and carbazole hydrazone. All synthesized carbazole derivatives were evaluated for their *in vitro* cytotoxic activity against 7901 (gastric adenocarcinoma), A875 (human melanoma) and MARC145 (African green monkey kidney) cell lines. The preliminary results indicated that compound **14a** exhibited high inhibitory activities on 7901 and A875 cancer cells with the lowest IC_{50} of 11.8 ± 1.26 and 9.77 ± 8.32 μM, respectively, which might be the new lead compound for discovery of novel carbazole-type anticancer agents.

1 Introduction

Cancer has long been an important disease threatening human health. Except the direct invasive therapy, radiotherapy, the use of chemotherapeutic drugs to kill cancer cells and treat tumors are the most important treatment of intermediate and advanced tumors with clinical metastasis (Sung et al., 2021). In the current clinical trials of cancer treatment, 65% of drugs are derived from natural products (Newman and Cragg, 2020; Bhutani et al., 2021). Despite the extensive use of drug design, compounds in nature are still the focus of drug research and development.

Natural products, especially heterocyclic compounds, have always been an important source of anticancer drugs and a molecular library of potential drugs (Fang et al., 2021; Yang et al., 2021). Many natural products or their derivatives have been demonstrated to have extensive antitumor activities by inducing apoptosis (Chen et al., 2015; Liu et al., 2015; Padmaja et al., 2015; Bailly, 2020; Greco et al., 2021) and inhibiting mitosis (Thomas et al., 2016; Davison and Sperry, 2017; Yokoyama et al., 2019). As an important class of aromatic heterocyclic compounds, carbazole alkaloid derivatives have long been used in medicinal chemistry (Murali et al., 2017; Sun et al., 2017; Zhou et al., 2018; Cao et al., 2019; Issa et al., 2019; Liu et al., 2019; Rassias et al., 2019; Liu et al., 2020; Liu et al., 2021; Wang et al., 2022), agrochemicals (Kong et al., 2016; Wang et al., 2017; Dang et al., 2018; Sun et al., 2020; Xie et al., 2020) and other fields. So, how to realize the functional modification of carbazole ring to improve its activity is always an important research direction.

In our previous work, a series of thirty carbazole arylhydrazone derivatives were conveniently synthesized and evaluated as potential cytotoxic agents, using two of the same cells as this paper, namely A875 (human melanoma) and MARC145 (African green monkey kidney cell line MA-104) cells. Among them, compound **2021-7e** (Figure 5) elicited the lowest IC$_{50}$ against A875 (4.15 μM) and IC$_{50}$ of 26.64 μM on MARC145 (Huang et al., 2021). Meanwhile, a three-components indole-to-carbazole reaction (Wu et al., 2021) was adopted to construct the carbazole scaffold, which has high yield compared to the traditional reactions (Aggarwal and Verma, 2019; Wu et al., 2021). However, the carbazole unit is directly connected with the carbonyl group forming a p-π rigid conjugated system, which may not be conducive to the binding with the receptor protein. So, in order to further investigate the derivatization ability and drug potential of carbazole analogues, a methylene unit was introduced to provide a rotatable bond attached to the carbazole scaffold (Figure 1), and a series of carbazole derivatives with structural diversity including carbazole amide, carbazole hydrazide and carbazole hydrazone were designed and synthesized. We hope that the introduction of this flexibility is proposed to increase the binding ability of target molecules to receptor proteins.

Thus, we wish to report herein the convenient synthesis of novel carbazole derivatives with structural diversity as indicated in Scheme 1, and their potential cytotoxic activities against several cell lines including human gastric adenocarcinoma cells (7901), human melanoma (A875), and a subclone of African green monkey kidney cell line MA-104 (MARC145) were investigated using classical MTT colorimetric method.

2 Results and discussion

2.1 Chemistry

In this work, three series of carbazole analogues with structural diversity were designed and synthesized by integrating the carbazole alkaloid moiety with diverse pharmacophores including amide, hydrazide and acylhydrazone *etc*. The general synthetic route and structures is depicted in Scheme 1.

In previous studies it was demonstrated that a series of carbazole structures could be obtained by the three-component reaction of bromoacetal acetal, ketone and indole catalyzed by bismuth trifluoromethanesulfonate (Gu et al., 2018), but the carbazole structure is directly connected to the carbonyl group, which formed a rigid conjugated structure. In order to further explore the potential effect of adding rotatable bonds to improve molecular flexibility on activity, different types of carbazole derivatives were designed and synthesized. Firstly, 1-methyl-9*H*-carbazoles **7a-e** were synthesized via three steps according to our previous procedure. The carbazole scaffold **5** was synthesized using indole, ethyl acetoacetate and 2-(bromomethyl)-1,3-dioxolane, which was then hydrolyzed to obtain the corresponding acids **6**, and then treated with a pharmacophore-bearing amine to form various amide derivatives. Similarly, the key carbazole acids with rotatable bonds of type **10** were constructed via three steps (Percy et al., 1994) as indicated in Scheme 1; In particular, the carbazole acetyl **8** was obtained using a similar method to compounds **5** by using ethyl acetoacetate instead of 4,4-dimethoxybutan-2-one. Therefore, the carbonyl group of compounds **8** was cyanated through trimethylcyanosilane, and then hydrolyzed to obtain the intermediate carbazole acids **10**, which were isolated as a white solid by column chromatography. A series of compounds **11a-e**

were conveniently synthesized by direct reaction of carbazole acids **10** with the appropriate amines. Compounds **10** were also transformed into the corresponding carbazole hydrazide **13** via two steps: esterification of the acid group followed by reaction with hydrazine hydrate. The compounds **13** were also reacted with a carbonyl-bearing substrate to obtain compounds **14a-g**, which bridges the carbazole structure to the potentially active pharmacophore (Popiolek et al., 2018; Xie et al., 2019; Duangdee et al., 2020; Han et al., 2020; Peng et al., 2020; Wang et al., 2020). Because the condensation method used is not stereoselective, the resulting acylhydrazone derivatives are a mixed (E/Z) configuration.

2.2 Spectroscopy

All obtained carbazole derivatives were elucidated based on the chemical analyses including ^{1}H NMR, ^{1}C NMR, ESI-MS, HRMS, and X-Ray analyses. For the ^{1}H NMR spectra of all 1-methyl-9*H*-carbazole derivatives **7a-e**, the obvious signals at 2.08–2.66 ppm were attributed to the methyl group attached to the carbazole ring as shown in the molecular structure. With respect to other carbazole derivatives **11a-e** and **14a-g**, the ^{1}H NMR spectrum indicated a unique signal for the flexible bond CHCH$_3$ unit, with a quartet signal at about 4.92–3.73 ppm and a doublet signal at about 1.63–1.40 ppm, respectively. Both the NH protons on the carbazole ring and the NH protons next to the carbonyl appear in the range of 11.52–9.56 ppm. The remaining signal peaks at low fields are attributed to the proton peaks of the carbazole ring or other aromatic rings. All the characteristic peaks observed within the ^{1}H NMR spectra for title compounds are given in materials and methods. In addition, the representative single crystal diffraction analysis of target compound **14a** is shown in Figure 2.

2.3 Pharmacology evaluation

Using 5-fluorouracil (5-FU) as a positive control, the inhibition effects of all carbazole derivatives on 7901 (gastric adenocarcinoma cells), A875 (human melanoma) and MARC145 (African green monkey kidney cell line MA-104) cells *in vitro* were evaluated by standard MTT assay, and the preliminary bioassay results were described in Figure 3. Generally, as shown in Figure 3, some compounds showed higher activities compared with the control 5-FU. Among them, carbazole derivatives **7b**, **11a**, **11b**, **14a**, and **14b** had higher *in vitro* inhibition rates on the two cancer cells 7901 and A875 (>70%). In addition, compounds **7b**, **11a** and **14a** had less toxicity to normal cells MARC-145 than cancer cells, especially, it is worth noting that, compound **14a** have little toxicity to normal cells MARC-145 and show moderate selectivity to cancer cells.

Through the preliminary screening results, some molecules showed good inhibitory effects on target cancer cells. In order to further verify the potential activity of these carbazole derivatives, we determined the IC$_{50}$ values of all compounds **7a-e**, **11a-e**, and **14a-g**. It is further proved that compounds **11a**, **11b**, **14a**, **14b** are the highly potential scaffolds with excellent anticancer activities.

Generally, the carbazole derivatives with flexible bonds attached to carbazole ring have some advantages compared with the carbazole derivatives with rigid structures, and overall exhibit better inhibitory activity against cancer cells. It is worth noting that compounds **11a**,
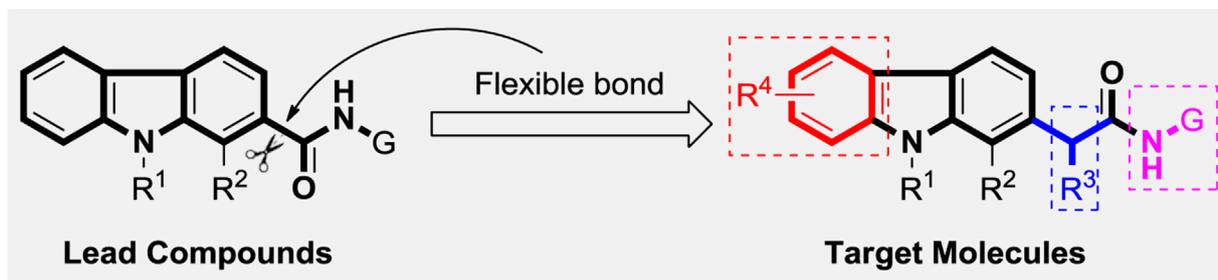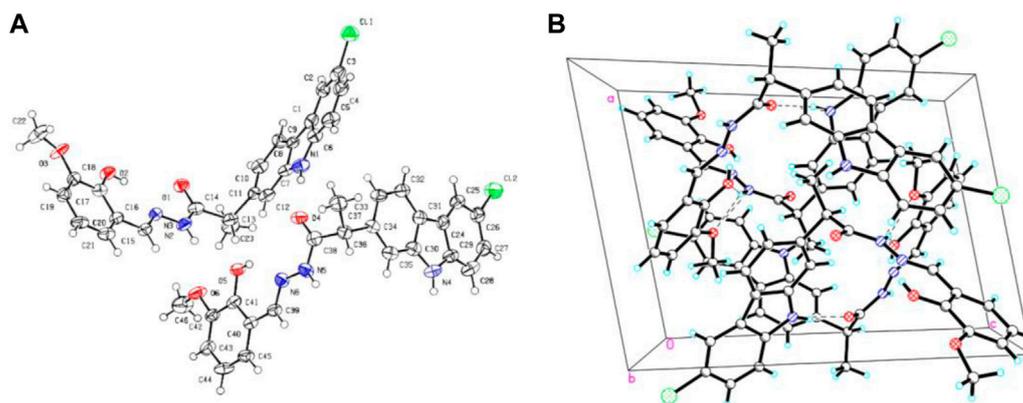
FIGURE 1
Design of novel carbazole alkaloid derivatives.
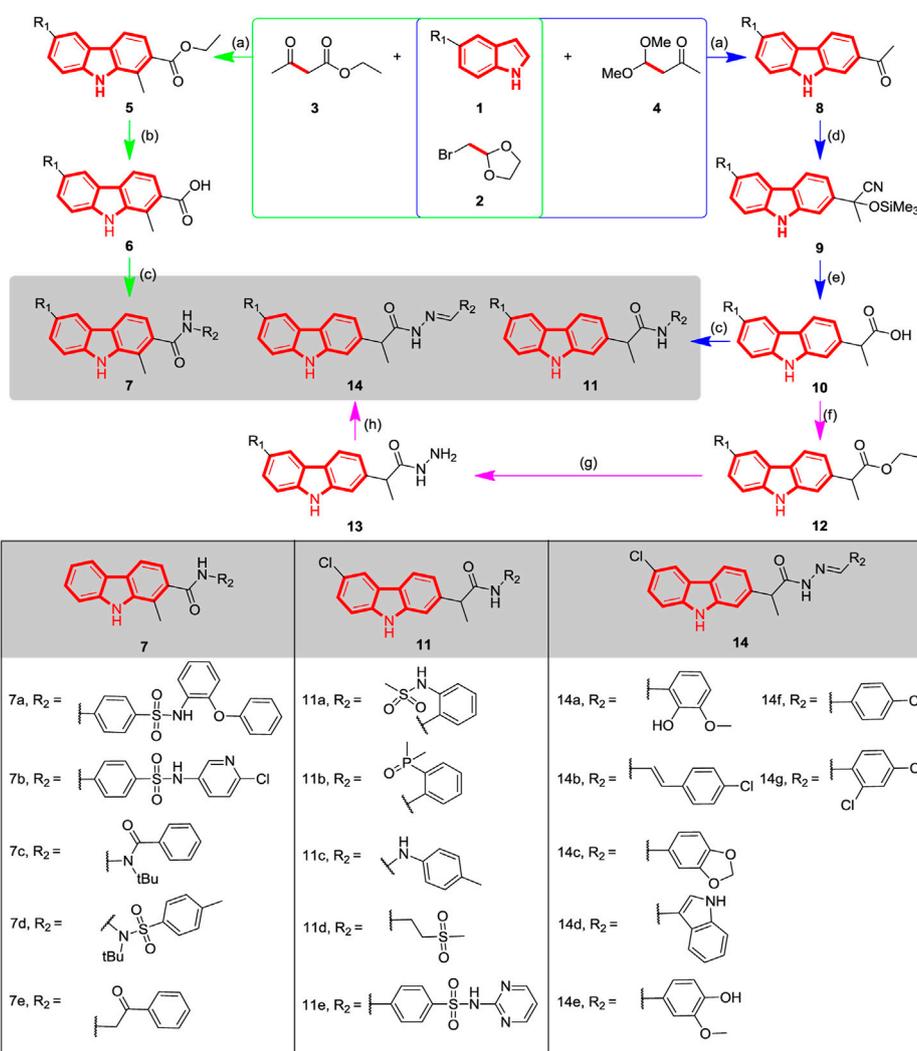
SCHEME 1
Synthetic route and structure of carbazole derivatives **7a-e**, **11a-e** and **14a-g**. Reagents and conditions: (a) AlCl₃, CH₃CN, reflux; (b) KOH, EtOH, rt; (c) i. Py, MsCl, CH₃CN, 0°C; ii. R₂-NH₂ or R₂=NNH₂, 40–50 °C; (d) Me₃SiCN, ZnI₂, rt; (e) i. SnCl₂, AcOH, rt; ii. conc. HCl; (f) EtOH, Conc. H₂SO₄, reflux; (g) NH₂NH₂·H₂O, EtOH, reflux; (h) Aldehyde, EtOH, reflux.

FIGURE 2
Single crystal structure **(A)** and packing diagram **(B)** for compound **14a**, and the dashed lines denote intermolecular hydrogen bonds.
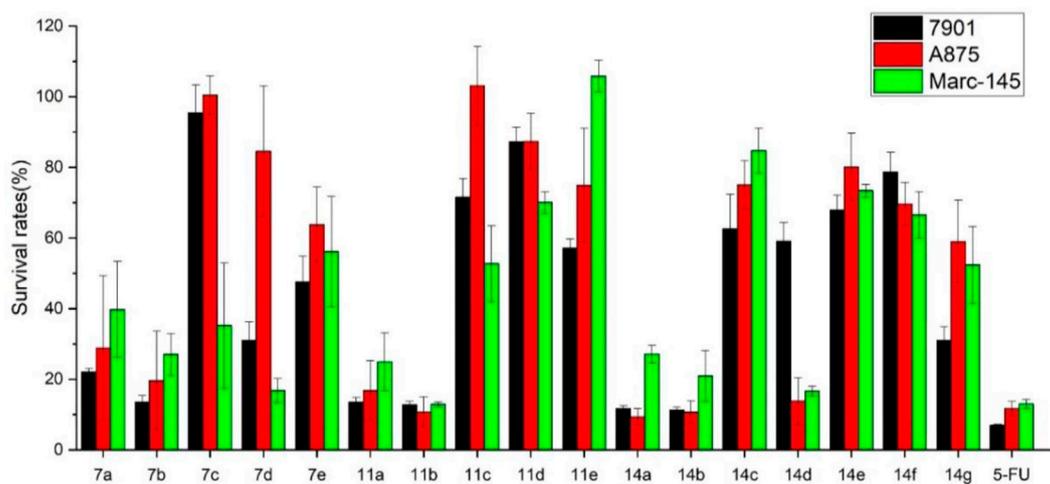
FIGURE 3
Cytotoxic activities of synthesized compounds at the concentration of 40 μg/mL. Abbreviations: 7901—Human gastric cancer cell line; A875—Human melanoma cell line; MARC145—A subclone of African green monkey kidney cell line MA-104; 5-FU—5-Fluorouracil, used as a positive control.
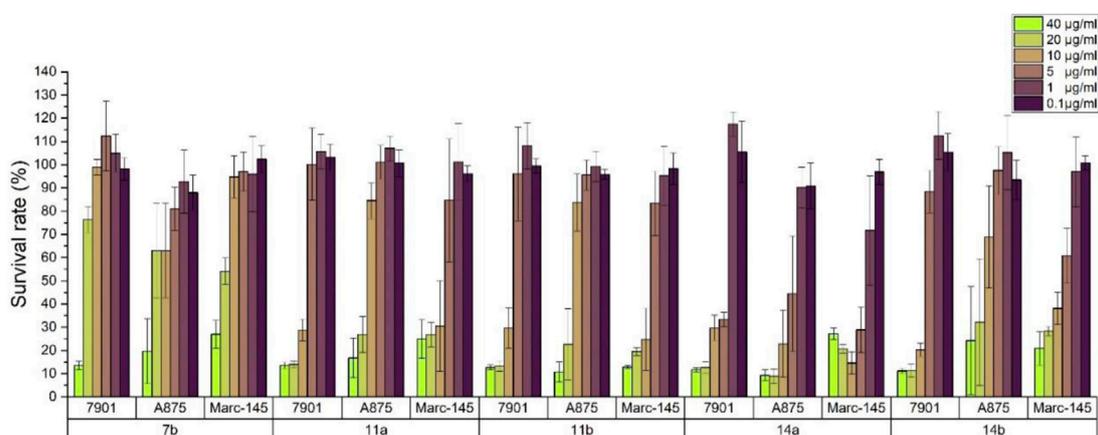
FIGURE 4
Survival rates of 7901, A875 and Marc-145 in different concentration of **7b**,**11a**, **11b**, and **14a**, **14b**.

TABLE 1 *In vitro* cytotoxic activities of target compounds against tested cell lines.

| Entry | Compd. No. | Substituents | | *In vitro* cytotoxicity IC$_{50}$[a] (µM) | | |
		R$_1$	R$_2$	7901[b]	A875[b]	MARC145[b]
1	**7a**	H		64.72 ± 15.12	33.53 ± 1.63	51.49 ± 9.24
2	**7b**	H		58.11 ± 11.26	23.04 ± 16.95	58.88 ± 16.68
3	**7c**	H		>40	>40	58.4 ± 31.59
4	**7d**	H		34.52 ± 9.9	>40	18.73 ± 4.16
5	**7e**	H		>40	>40	62.59 ± 28.21
6	**11a**	Cl		21.9 ± 3.05	36.68 ± 2.96	22.94 ± 14.3
7	**11b**	Cl		20.57 ± 3.3	33.62 ± 9.48	17.32 ± 7.25
8	**11c**	Cl		>40	>40	63.96 ± 20.11
9	**11d**	Cl		>40	>40	>40
10	**11e**	Cl		>40	>40	>40
11	**14a**	Cl		11.8 ± 1.26	9.77 ± 8.32	7.47 ± 4.15
12	**14b**	Cl		18.95 ± 2.64	45.56 ± 30.64	19.57 ± 6.94
13	**14c**	Cl		>40	>40	>40
14	**14d**	Cl		>40	37.58 ± 8.15	42.44 ± 4.58
15	**14e**	Cl		>40	>40	>40
16	**14f**	Cl		>40	>40	>40
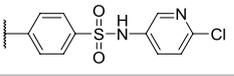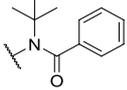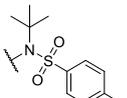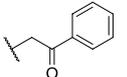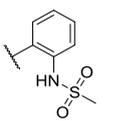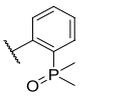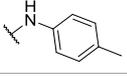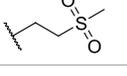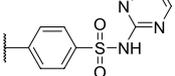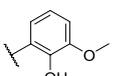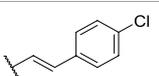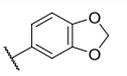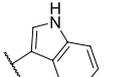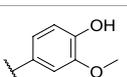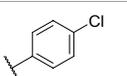
TABLE 1 (*Continued*) *In vitro* cytotoxic activities of target compounds against tested cell lines.

Entry	Compd. No.	Substituents		*In vitro* cytotoxicity IC$_{50}$[a] (μM)		
		R$_1$	R$_2$	7901[b]	A875[b]	MARC145[b]
17	**14g**	Cl	(2,4-dichlorophenyl structure)	38.83 ± 2.74	>40	96.26 ± 63.3
18	**5-FU**[c]	-	-	63.5 ± 4.92	80.11 ± 6.61	86.33 ± 8.3

[a]IC$_{50}$, Compound concentration required to inhibit tumor cell proliferation by 50%.
[b]Abbreviations: 7901, Human gastric carcinoma cell line; A875, Human melanoma cell line; MARC145, A subclone of African green monkey kidney cell line MA-104.
[c]Used as a positive control.

FIGURE 5
General structure-activity profile for these carbazole derivatives and previous work.
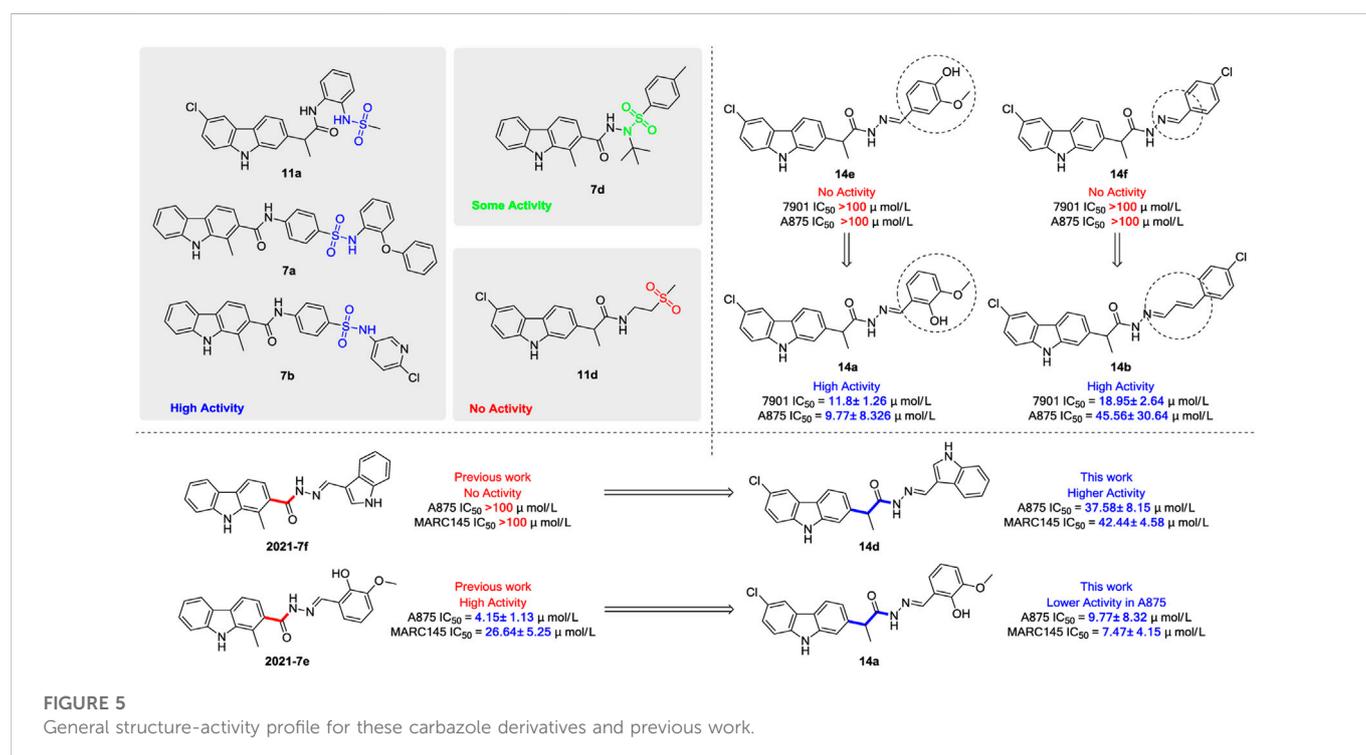
11b, **14a**, and **14b** exhibited good inhibition activities on all tested cells. Especially, compound **14a** derived from *o*-vanillin was most active molecule against all tested cell lines with the IC$_{50}$ value of 11.8, 9.77, and 7.47 μM, respectively, which was significantly better than that of the control 5-FU. However, compound **1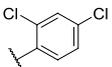4e** containing vanillin scaffold almost lost its activity, which indicated the hydrophilic groups in the neighborhood of the aromatic ring might be very important for the activity of these class of compounds. In addition, the four compounds **11a**, **11b**, **14a**, **14b** have similar structures to carprofen and may act as a pharmacophore to enhance its antitumor activity (Favia et al., 2012; Mellini et al., 2012; Zhou et al., 2018).

The relationship between concentration and inhibition rate is the key to whether a potential compound can be use as potential medicinal agents. It is very important to maintain good activity at low concentration. Based on the preliminary screening data, in order to verify the effect of concentration on the potential cytotoxic activities for all compounds, the inhibition activity data of the compounds at different concentrations were detected using the same method. All experiments were carried out on three kinds of cell lines with six

concentrations of 40, 20, 10, 5, 1, and 0.5 μg/mL. The inhibition activities for highly potential compounds 7b, 11a, 11b, 14a, and 14b were described in Figure 4. It can be seen that with the decrease of the concentration, the inhibition rate of the cells also decreased, but good activity was also guaranteed for compound **14a** at a concentration of 5 μg/mL, which was significantly better than that of other compounds tested.

The structure evolution here was to modify carbazole scaffold and different pharmacophore. According to the *in vitro* results described in Table 1, the possible structure-activity relationships for these synthesized carbazole derivatives can be concluded. Considering the type of pharmacophore, it can be clearly seen that the sulfonamide group can efficiently improve the potential activities of these compounds as indicated in Figure 5. When there is no hydrogen on the amino group, the compound's activity (such as 7d) decreases significantly, as it may affect the formation of hydrogen bonds. However, the molecule **11d** containing only sulfone group also lost activity. The structural isomerism and the length of the carbon chain significantly affected the activity of

the compound. For example, the activity of compound **14a** bearing 2-hydroxy-3-methoxybenzylidene unit is significantly better than that of compound **14e** containing 4-hydroxy-3-methoxybenzylidene moiety, as well as for compound **14b** characterized with one more vinyl group than derivative **14f**. In contrast to the previous work, the addition of flexible bonds produced complex effects. On the one hand, the activity of some compounds was improved (such as **14d**), likely due to the increase of rotatable bonds which i) reduced the permeability to the cell membrane, or ii) increased the entropy penalty when binding proteins. However, the rotatable bonds also reduced the activity of some compounds (for example, compounds **14a**). It is worth noting that the 2-hydroxy-3-methoxybenzylidene group is the most effective pharmacophore in the previous work (Compound **2021-7e**) and this work (Compound **14a**), and has the value of further research (Huang et al., 2021) (Figure 5).

According to the aforementioned analysis, the potential inhibitor activity is relatively good for those carbazole derivatives with higher molecular flexibility. In the rigid structure, only **7b** has moderate inhibitory activity on tested cells, which reflects the effect of molecular flexibility on the activity of these compounds. The increase of rotatable bonds may facilitate the binding of compounds to possible receptors, so as to improve its inhibitory activity (Peng et al., 2019; Caron et al., 2020).

3 Conclusion

In this study, several types of carbazole derivatives including carbazole amides, carbazole hydrazides and carbazole hydrazones were designed and synthesized based on the scaffold of carbazole alkaloids. All obtained molecules were fully characterized by ^{1}H NMR, ^{13}C NMR, ESI-MS, HRMS and X-Ray diffraction analyses, and their potential inhibitory activities on cancer cell lines were bio-evaluated. The bioassay indicated that some of the target compounds had good inhibitory effects on 7901 and A875 cancer cells, especially, the best potential compound **14a** exhibited high inhibitory activities with the lowest IC$_{50}$ of 11.8 ± 1.26 and 9.77 ± 8.32 μM, respectively, which might be the new lead molecule for discovery of novel carbazole-type anticancer agents.

4 Materials and methods

4.1 Instrumentation and chemicals

All melting points (m.p.) were measured using a digital model X-5 apparatus and are uncorrected. ^{1}H NMR and ^{13}C NMR spectra were recorded on a Bruker Avance III 600 MHz FT-NMR spectrometer using DMSO-d_6 as the solvent and tetramethylsilane (TMS) as the internal standard. Mass spectra were performed on a WATERS ACQUITY UPLC$^®$ H-CLASS PDA (Waters$^®$) instrument. High resolution mass spectrometry analysis (HRMS) was done with Agilent 6224 TOF mass spectrometer. Thin-layer chromatography was carried out on precoated silica gel plates GF254 (Qingdao Haiyang Chemical, China), and spots were visualized with ultraviolet light. All starting materials and reagents commercially available were used without further purification, unless otherwise specified.

4.2 General synthetic procedure for 1-methyl-9H-carbazole-2-carboxylic acid **6**

Indole (10.0 mmol), ethyl acetoacetate (10.0 mmol), 2-(bromomethyl)-1,3-dioxolane (12.0 mmol), AlCl$_3$ (0.5 mmol, 5 mol %) and acetonitrile (35 mL) was added in a 100 mL single-neck flask. The mixture was stirred at 80°C for 6 h obtaining a solid which was filtered under reduced pressure. The residue product was rinsed by brine, and the aqueous phase was extracted by ethyl acetate. The organic phase was combined, dried over anhydrous Na$_2$SO$_4$ and filtered. The solvent was removed by rotary evaporation to obtain the crude intermediate **5**. The latter was added in a 100 mL single-neck flask with methanol (10 mL) and sodium hydroxide (15 mmol), and the reaction was stirred at room temperature overnight. The mixture was added dilute hydrochloric acid adjust to pH 2-3 under ice-bath, and the precipitate was 1-methyl-9H-carbazole-2-carboxylic acid **6**. The compound was brown powder, MS (ESI) m/z calcd for C$_{14}$H$_{10}$NO$_2$ [M - H]$^-$ 224.08, found 224.48.

4.3 General synthetic procedure for 2-(6-chloro-9H-carbazol-2-yl)propanoic acid **10**

Indole (10.0 mmol), 4,4-dimethoxybutan-2-one (10.0 mmol), 2-(bromomethyl)-1,3-dioxolane (12.0 mmol), AlCl$_3$ (0.5 mmol, 5 mol %) and acetonitrile (35 mL) was added in a 100 mL single-neck flask. The mixture was stirred at 80°C for 8 h. After reaction, the solid was filtered under reduced pressure. The residue product was rinsed by brine, and the aqueous phase was extracted by ethyl acetate, then combine the residue and the organic phase, which was dried over anhydrous Na$_2$SO$_4$. After that, the solvent was removed by rotary evaporation, and the residue was used directly in subsequent reactions without purification. The residue was added in a 100 mL single-neck flask, and treated with trimethylsilyl cyanide and ZnI$_2$ under the condition of reflux. After reaction, the mixture was cooled to room temperature and filtered, which was concentrated to obtain crude product **9**. Subsequently, compounds **9** was treated with stannous chloride in acetic acid, then hydrolysis with concentrated hydrochloric acid, and the carbazole derivative 2-(6-chloro-9H-carbazol-2-yl) propanoic acid **10** will be obtained through a series of acid-base treatment. MS (ESI) m/z calcd for C$_{15}$H$_{12}$ClNO$_2$ [M - H]$^-$ 272.06, found 272.41.

4.4 General synthetic procedure for 2-(6-chloro-9H-carbazol-2-yl) propanehydrazide **13**

To a solution of substituted 2-(6-chloro-9H-carbazol-2-yl) propanoic acid **10** (10 mmol) in ethanol was added the catalytic amount of concentrated sulfuric acid, which was refluxed at 80°C for 6-7 h. Then, the solution was washed with water and extracted with ethyl acetate, and the organic phase was directly used for the next reaction after drying and concentration. The residue was dissolved in 10 mL of ethanol, and 5 eq. of hydrazine hydrate was added, the mixture was heated at 70-75°C for 4 h. The precipitate was filtered and washed with a small amount of cold ethanol to obtain the desired molecule 2-(6-chloro-9H-carbazol-2-yl)propanehydrazide **13**: MS (ESI) m/z calcd for C$_{15}$H$_{14}$ClN$_3$O [M + H]$^+$ 288.08, found 288.25.

4.5 General synthetic procedure for the target compounds **7a-e** and **11a-e**

The general synthetic procedure of carbazole-based amide **7a-e** and **11a-e**: To a solution of carbazole-based carboxylic acids **6** or **10** (0.8 mmol) in 10 mL anhydrous acetonitrile was added pyridine (2.4 mmol) under the condition of 0–5°C. Then, methanesulfonyl chloride (1.2 mmol) was added dropwise to the mixture, which was then allowed to warm to room temperature and stirred for additional half hour, the various amines (0.8 mmol) were added, and the reaction mixture was heated to 40–45°C and detected by thin-layer chromatography. After completion of the reaction, the mixture was quenched by the addition of water, and the suspended solid was collected by filtration and washed with water to afford the crude products, which were purified by silica gel column chromatography (petroleum ether/ethyl acetate) to give the target compounds. Their physico-chemical properties and the spectra data are as follows:

1-Methyl-N-(4-(N-(2-phenoxyphenyl)sulfamoyl)phenyl)-9H-carbazole-2-carboxamide (**7a**): white solid; yield: 71%; m. p. 78°C; ^{1}H NMR (600 MHz, DMSO-d_6, 25°C) δ = 11.42 (s, 1H), 10.69 (s, 1H), 9.87 (s, 1H), 8.17 (d, J = 7.8 Hz, 1H), 8.08 (d, J = 8.0 Hz, 1H), 7.87—7.82 (m, 2H), 7.71—7.66 (m, 2H), 7.56 (dt, J = 8.1, 0.9 Hz, 1H), 7.46—7.40 (m, 2H), 7.33—7.29 (m, 3H), 7.21—7.18 (m, 1H), 7.12—7.08 (m, 3H), 6.75—6.71 (m, 1H), 6.71—6.67 (m, 2H), 2.65 (s, 3H) ppm; ^{13}C NMR (151 MHz, DMSO-d_6, 25°C) δ = 169.26, 156.62, 149.93, 143.65, 141.11, 139.65, 133.74, 130.22, 130.15, 128.27, 126.64, 125.95, 124.07, 123.84, 123.56, 122.77, 121.23, 119.59, 119.40, 119.00, 118.98, 118.93, 118.66, 117.94, 111.77, 40.39, 40.26, 40.12, 39.98, 39.84, 39.70, 39.56, 14.82, 0.59 ppm; MS (ESI) m/z 548.38 = [M + H]$^+$, HRMS m/z 548.1633 = [M + H]$^+$, calcd. for $C_{32}H_{25}N_3O_4S$ m/z = 547.1566.

N-(4-(N-(6-Chloropyridin-3-yl)sulfamoyl)phenyl)-1-methyl-9H-carbazole-2-carboxamide (**7b**): brown solid; yield: 56%; m. p. 93°C; ^{1}H NMR (600 MHz, DMSO-d_6, 25°C) δ = 11.41 (s, 1H), 10.76 (s, 1H), 10.68 (s, 1H), 8.16 (d, J = 7.7 Hz, 1H), 8.13 (d, J = 2.9 Hz, 1H), 8.06 (d, J = 8.0 Hz, 1H), 7.99—7.94 (m, 2H), 7.78 (d, J = 8.9 Hz, 2H), 7.59 (dd, J = 8.7, 2.9 Hz, 1H), 7.55 (d, J = 8.1 Hz, 1H), 7.44 (d, J = 8.5 Hz, 2H), 7.31 (d, J = 8.0 Hz, 1H), 7.22—7.17 (m, 1H), 2.62 (s, 3H) ppm; MS (ESI) m/z 491.45 = [M + H]$^+$, HRMS m/z 491.0922 = [M + H]$^+$, calcd. for $C_{25}H_{19}ClN_4O_3S$ m/z = 490.0866.

N'-Benzoyl-N'-(tert-butyl)-1-methyl-9H-carbazole-2-carbohydrazide (**7c**): white solid; yield: 79%; m. p. 212°C; ^{1}H NMR (600 MHz, DMSO-d_6, 25°C) δ = 11.23 (s, 1H), 10.53 (s, 1H), 8.08 (d, J = 7.8 Hz, 1H), 7.87 (d, J = 8.0 Hz, 1H), 7.51—7.47 (m, 3H), 7.44—7.36 (m, 4H), 7.16—7.13 (m, 1H), 6.52 (d, J = 8.0 Hz, 1H), 2.08 (s, 3H), 1.55 (s, 9H) ppm; ^{13}C NMR (151 MHz, DMSO-d_6, 25°C) δ = 172.62, 168.54, 140.91, 139.46, 138.59, 131.17, 129.71, 128.01, 127.37, 126.62, 123.45, 122.63, 121.14, 119.33, 119.21, 117.70, 117.56, 111.68, 60.59, 28.06, 13.74 ppm; MS (ESI) m/z 422.40 = [M + Na]$^+$, HRMS m/z 400.2014 = [M + H]$^+$, calcd. for $C_{25}H_{25}N_3O_2$ m/z = 399.1947.

N-(tert-Butyl)-4-methyl-N'-(1-methyl-9H-carbazole-2-carbonyl) benzenesulfonohydrazide (**7d**): yellow solid; yield: 85%; m. p. 97°C; ^{1}H NMR (600 MHz, DMSO-d_6, 25°C) δ = 11.33 (s, 1H), 10.31 (s, 1H), 8.14 (d, J = 7.7 Hz, 1H), 8.02—8.00 (m, 3H), 7.54 (d, J = 7.9 Hz, 1H), 7.44—7.40 (m, 3H), 7.20—7.13 (m, 2H), 2.39 (s, 3H), 1.40 (d, J = 3.2 Hz, 9H) ppm; ^{13}C NMR (151 MHz, DMSO-d_6, 25°C) δ = 169.98, 143.70, 141.00, 139.59, 139.32, 131.78, 129.74, 128.36, 126.58, 123.51, 122.76, 121.15, 119.34, 118.74, 117.59, 111.73, 63.29, 28.79, 21.50, 14.51 ppm; MS (ESI) m/z 450.23 = [M + H]$^+$, HRMS m/z 450.1836 = [M + H]$^+$, calcd. for $C_{25}H_{27}N_3O_3S$ m/z = 449.1773.

1-Methyl-N-(2-oxo-2-phenylethyl)-9H-carbazole-2-carboxamide (**7e**): yellow solid; yield: 67%; m. p. 153°C; ^{1}H NMR (600 MHz, DMSO-d_6) δ = 11.32 (s, 1H), 8.59 (t, J = 5.7 Hz, 1H), 8.15—8.00 (m, 4H), 7.72—7.67 (m, 1H), 7.61—7.53 (m, 3H), 7.44—7.41 (m, 1H), 7.28 (d, J = 8.0 Hz, 1H), 7.19—7.17 (m, 1H), 4.80 (d, J = 5.8 Hz, 2H), 2.66 (s, 3H) ppm; ^{13}C NMR (151 MHz, DMSO) δ = 196.02, 170.49, 140.97, 139.75, 135.63, 134.01, 133.87, 129.32, 128.37, 126.38, 123.12, 122.88, 121.05, 119.28, 119.03, 118.63, 117.69, 111.70, 46.92, 14.75 ppm; MS (ESI) m/z 343.33 = [M + H]$^+$, HRMS m/z 343.1469 = [M + H]$^+$, calcd. for $C_{22}H_{18}N_2O_2$ m/z = 342.1368.

2-(6-Chloro-9H-carbazol-2-yl)-N-(2-(methylsulfonamido) phenyl)propanamide (**11a**): yellow solid; yield: 64%; m. p. 163°C; ^{1}H NMR (600 MHz, DMSO-d_6, 25°C) δ = 11.39 (s, 1H), 9.56 (s, 1H), 8.79 (s, 1H), 8.18 (d, J = 2.1 Hz, 1H), 8.11 (d, J = 8.1 Hz, 1H), 7.64 (dd, J = 8.1, 1.5 Hz, 1H), 7.54—7.51 (m, 1H), 7.48 (dd, J = 8.5, 0.5 Hz, 1H), 7.36 (dd, J = 8.6, 2.1 Hz, 1H), 7.33 (dd, J = 7.9, 1.6 Hz, 1H), 7.25—7.22 (m, 2H), 7.17 (td, J = 7.7, 1.6 Hz, 1H), 4.07 (q, J = 7.0 Hz, 1H), 2.64 (s, 3H), 1.53 (d, J = 7.0 Hz, 3H) ppm; MS (ESI) m/z 442.48 = [M + H]$^+$, HRMS m/z 442.0985 = [M + H]$^+$, calcd. for $C_{22}H_{20}ClN_3O_3S$ m/z = 441.0914.

2-(6-Chloro-9H-carbazol-2-yl)-N-(2-((dimethylphosphoryl) amino)phenyl)propanamide (**11b**): yellow solid; yield: 77%; m. p. 148°C; ^{1}H NMR (600 MHz, DMSO-d_6, 25°C) δ = 11.79 (s, 1H), 11.41 (s, 1H), 8.42 (dd, J = 8.5, 3.9 Hz, 1H), 8.17 (d, J = 2.1 Hz, 1H), 8.10 (d, J = 8.1 Hz, 1H), 7.53 (ddd, J = 13.8, 7.7, 1.6 Hz, 1H), 7.51—7.46 (m, 3H), 7.36 (dd, J = 8.6, 2.1 Hz, 1H), 7.20 (dd, J = 8.1, 1.5 Hz, 1H), 7.14—7.10 (m, 1H), 3.82 (q, J = 7.0 Hz, 1H), 1.77 (d, J = 13.6 Hz, 3H), 1.62 (d, J = 13.5 Hz, 3H), 1.54 (d, J = 7.0 Hz, 3H) ppm; ^{13}C NMR (151 MHz, DMSO-d_6, 25°C) δ = 172.56, 143.62, 143.60, 141.05, 140.28, 138.81, 132.93, 131.27, 131.20, 125.59, 124.04, 123.32, 121.21, 121.02, 120.15, 119.11, 112.82, 110.19, 48.74, 18.78 ppm; MS (ESI) m/z 425.38 = [M + H]$^+$, HRMS m/z 425.1176 = [M + H]$^+$, calcd. for $C_{23}H_{23}ClN_3O_2P$ m/z = 424.1216.

2-(6-Chloro-9H-carbazol-2-yl)-N'-(p-tolyl)propanehydrazide (**11c**): white solid; yield: 88%; m. p. 188°C; ^{1}H NMR (600 MHz, DMSO-d_6, 25°C) δ = 11.38 (s, 1H), 9.83 (d, J = 3.2 Hz, 1H), 8.18 (d, J = 2.1 Hz, 1H), 8.09 (d, J = 8.1 Hz, 1H), 7.55 (d, J = 3.2 Hz, 1H), 7.51—7.46 (m, 2H), 7.36 (dd, J = 8.6, 2.2 Hz, 1H), 7.19 (dd, J = 8.2, 1.5 Hz, 1H), 6.84 (d, J = 8.1 Hz, 2H), 6.51—6.47 (m, 2H), 3.85 (q, J = 7.0 Hz, 1H), 2.12 (s, 3H), 1.46 (d, J = 7.0 Hz, 3H) ppm; ^{13}C NMR (151 MHz, DMSO-d_6, 25°C) δ = 173.63, 147.59, 141.02, 140.74, 138.80, 129.48, 127.40, 125.47, 124.14, 123.28, 120.87, 120.81, 120.12, 119.30, 112.80, 112.65, 110.13, 44.17, 20.54, 19.10 ppm; MS (ESI) m/z 378.18 = [M + H]$^+$, HRMS m/z 378.1366 = [M + H]$^+$, calcd. for $C_{22}H_{20}ClN_3O$ m/z = 377.1295.

2-(6-Chloro-9H-carbazol-2-yl)-N-(2-(methylsulfonyl)ethyl) propanamide (**11d**): white solid; yield: 73%; m. p. 149°C; ^{1}H NMR (600 MHz, DMSO-d_6, 25°C) δ = 11.38 (s, 1H), 8.31 (t, J = 5.7 Hz, 1H), 8.17 (d, J = 2.1 Hz, 1H), 8.06 (d, J = 8.1 Hz, 1H), 7.48 (d, J = 8.5 Hz, 1H), 7.43 (d, J = 1.4 Hz, 1H), 7.36 (dd, J = 8.6, 2.2 Hz, 1H), 7.13 (dd, J = 8.2, 1.5 Hz, 1H), 3.75 (q, J = 7.0 Hz, 1H), 3.47—3.40 (m, 2H), 3.25—3.17 (m, 2H) 2.90 (s, 3H), 1.41 (d, J = 7.0 Hz, 3H) ppm; ^{13}C NMR (151 MHz, DMSO) δ = 174.26, 141.01, 140.95, 138.77, 125.46, 124.11, 123.26, 120.92, 120.75, 120.07, 119.26, 112.78, 110.12, 53.45, 46.02, 41.22, 33.35, 19.39 ppm; MS (ESI) m/z 378.90 = [M + H]$^+$, HRMS m/z 379.0872 = [M + H]$^+$, calcd. for $C_{18}H_{19}ClN_2O_3S$ m/z = 378.0805.

2-(6-Chloro-9H-carbazol-2-yl)-N-(4-(N-(pyrimidin-2-yl) sulfamoyl)phenyl)propanamide (**11e**): yellow solid; yield: 65%; m. p. 157°C; ^{1}H NMR (600 MHz, DMSO-d_6, 25°C) δ = 11.37 (s, 1H),

10.49 (s, 1H), 8.46 (d, J = 4.9 Hz, 2H), 8.15 (d, J = 2.1 Hz, 1H), 8.08 (d, J = 8.1 Hz, 1H), 7.91—7.88 (m, 2H), 7.79—7.75 (m, 2H), 7.50—7.45 (m, 2H), 7.35 (dd, J = 8.6, 2.1 Hz, 1H), 7.20 (dd, J = 8.2, 1.5 Hz, 1H), 7.01 (t, J = 4.9 Hz, 1H), 4.00 (q, J = 6.9 Hz, 1H), 1.49 (d, J = 6.9 Hz, 3H) ppm; ^{13}C NMR (151 MHz, DMSO) δ = 173.53, 157.37, 143.61, 141.02, 140.41, 138.80, 129.86, 129.33, 125.57, 124.05, 123.32, 121.11, 120.94, 120.12, 119.15, 118.93, 117.89, 112.81, 110.08, 46.99, 19.44 ppm; MS (ESI) m/z 506.31 = [M + H]$^+$, HRMS m/z 506.1039 = [M + H]$^+$, calcd. for $C_{25}H_{20}ClN_5O_3S$ m/z = 505.0975.

4.6 General synthetic procedure for the target compounds 14a-g

The general procedure for the synthesis of carbazole hydrazones **14a-g**: Various aldehyde (0.55 mmol) were added to solutions of substituted carbazole-based carbohydrazides **13** (0.5 mmol) in EtOH (6 mL), and then the mixtures were heated at reflux. After completion of reaction, the corresponding precipitation were collected by filtration, and washed with small amount of alcohol to give crude compounds, which were purified by flash chromatography and characterized by ESI-MS, HRMS, ^{1}H NMR and ^{13}C NMR spectra. Most of the obtained acylhydrazone derivatives are a mixed (E/Z) configuration, and so the NMR data of the mixture are linked with "and" in the follows.

2-(6-Chloro-9H-carbazol-2-yl)-N'-(2-hydroxy-3-methoxybenzylidene)propanehydrazide (**14a**): white solid; yield: 79%; m. p. 217°C; ^{1}H NMR (600 MHz, DMSO-d_6, 25°C) δ = 8.30 (s, 1H), 8.00—7.97 (m, 2H), 7.81—7.79 (m, 2H), 7.52—7.50 (m, 1H), 7.38 (d, J = 8.6 Hz, 1H), 7.31 (d, J = 2.0 Hz, 1H), 7.21 (dd, J = 8.2, 1.5 Hz, 1H), 7.02 (dd, J = 7.8, 1.4 Hz, 1H), 6.97 (dd, J = 8.1, 1.4 Hz, 1H), 6.84 (t, J = 8.0 Hz, 1H), 3.89 (s, 1H), 3.86 (s, 3H), 1.63—1.61 (m, 3H) ppm; ^{13}C NMR (151 MHz, DMSO-d_6, 25°C) δ = 170.11, 148.34, 147.44 and 147.40, 146.30, 141.04, 140.35, 138.81, 125.57, 124.07, 123.32, 121.10, 120.95, 120.14, 119.43, 119.32, 119.25, 114.15, 113.23 and 112.75, 112.82, 110.11, 56.25, 44.83, 19.36 ppm; MS (ESI) m/z 422.41 = [M + H]$^+$, HRMS m/z 422.1257 = [M + H]$^+$, calcd. for $C_{23}H_{20}ClN_3O_3$ m/z = 421.1193.

2-(6-Chloro-9H-carbazol-2-yl)-N'-(3-(4-chlorophenyl)allylidene)propanehydrazide (**14b**): white solid; yield: 82%; m. p. 186°C; ^{1}H NMR (600 MHz, DMSO-d_6, 25°C) δ = 11.46 and 11.32 (s, 1H), 11.37 and 11.24 (s, 1H), 8.17 and 8.15 (d, J = 2.1 Hz, 1H), 8.09 and 8.07 (d, 8.1 Hz, 1H), 7.96 and 7.77 (dd, J = 6.0, 2.4 Hz, 1H), 7.62 (dd, J = 10.1, 7.8 Hz, 2H), 7.49—7.41 (m, 4H), 7.35 (td, J = 8.8, 2.2 Hz, 1H), 7.17 (dt, J = 8.2, 1.4 Hz, 1H), 7.00—6.95 (m, 2H), 1.46 (t, J = 7.3 Hz, 3H) ppm; ^{13}C NMR (151 MHz, DMSO-d_6, 25°C) δ = 170.26, 148.69, 141.02, 140.58, 138.80, 137.26, 130.13, 129.29, 129.18, 129.14, 126.87, 121.04, 120.93, 120.12, 112.81, 110.07, 44.89, 40.40, 40.27, 40.13, 39.99, 39.85, 39.71, 39.57, 29.55, 29.49, 29.04, 22.56, 19.45 and 19.07 ppm; MS (ESI) m/z 436.34 = [M + H]$^+$, HRMS m/z 436.0976 = [M + H]$^+$, calcd. for $C_{24}H_{19}Cl_2N_3O$ m/z = 435.0905.

N'-(Benzo[d][1,3]dioxol-5-ylmethylene)-2-(6-chloro-9H-carbazol-2-yl)propanehydrazide (**14c**): white solid; yield: 84%; m. p. 240°C; ^{1}H NMR (600 MHz, DMSO-d_6, 25°C) δ = 11.45 and 11.37 (s, 1H), 11.34 and 11.18 (s, 1H), 8.15 and 814 (d, J = 2.1 Hz, 1H), 8.11 and 7.82 (s, 1H), 8.07 and 8.06 (d, J = 8.1 Hz, 1H), 7.49—7.44 (m, 2H), 7.35 (m, 1H), 7.29 and 7.21 (d, J = 1.6 Hz, 1H), 7.20—7.18 (m, 1H), 7.11 and 7.06 (dd, J = 8.0, 1.6 Hz, 1H), 6.95 (d, J = 5.5 Hz, 1H), 6.09 (d, J = 1.0 Hz, 1H), 6.07 (d, J = 1.0 Hz, 1H), 4.82 and 3.83 (q, J = 7.0 Hz, 1H), 1.47 (d, J = 7.0 Hz, 3H) ppm; ^{13}C NMR (151 MHz, DMSO-d_6, 25°C)

δ = 175.43 and 170.17, 149.44 and 149.19, 148.44 and 148.38, 146.83 and 142.78, 141.20 and 141.06, 141.03 and 140.63, 138.80 and 138.73, 129.25 and 129.14, 125.53 and 125.43, 124.10 and 124.09, 123.57 and 123.34, 123.30 and 123.24, 121.01 and 120.96, 120.87 and 120.64, 120.11 and 120.04, 119.61 and 119.26, 112.80 and 112.74, 110.15 and 110.08, 108.88 and 105.53 and 105.29, 101.97 and 101.93, 44.90 and 41.53, 19.49 and 19.38 ppm; MS (ESI) m/z 442.01 = [M + Na]$^+$, HRMS m/z 420.1110 = [M + H]$^+$, calcd. for $C_{23}H_{18}ClN_3O_3$ m/z = 419.1037.

N'-((1H-Indol-3-yl)methylene)-2-(6-chloro-9H-carbazol-2-yl)propanehydrazide (**14d**): white solid; yield: 78%; m. p. 209°C; ^{1}H NMR (600 MHz, DMSO-d_6, 25°C) δ = 11.52 and 11.49 (d, J = 2.7 Hz, 1H), 11.37 and 11.32 (s, 1H), 11.20 and 11.00 (s, 1H), 8.36 and 8.13 (s, 1H), 8.21—8.11 (m, 2H), 8.09—8.05 (d, J = 8.1 Hz, 1H), 7.75 and 7.71 (d, J = 2.8 Hz, 1H), 7.52 and 7.50 (s, 1H), 7.47 and 7.44 (d, J = 0.5 Hz, 1H), 7.43—7.40 (m, 1H), 7.35 and 7.32 (dd, J = 8.6, 2.2 Hz, 1H), 7.27—7.20 (m, 2H), 7.19—7.09 (m, 2H), 4.91 and 3.84 (q, J = 7.0 Hz, 1H), 1.51 (d, J = 3.5 Hz, 3H) ppm; ^{13}C NMR (151 MHz, DMSO-d_6, 25°C) δ = 174.75 and 169.51, 144.17 and 141.37, 141.07 and 141.05, 141.02 and 140.76, 138.80 and 138.73, 137.47 and 137.44, 130.59 and 130.54, 125.48 and 125.39, 124.74 and 124.51, 124.12, 123.27 and 123.21, 123.01, 122.35 and 122.09, 120.95 and 120.80, 120.73 and 120.61, 120.09 and 120.00, 119.57 and 119.33, 112.78 and 112.71, 112.30 and 112.23, 112.05 and 111.96, 110.10 and 110.06, 44.88 and 41.46, 19.75 and 19.49 ppm; MS (ESI) m/z 415.26 = [M + H]$^+$, HRMS m/z 415.1324 = [M + H]$^+$, calcd. for $C_{24}H_{19}ClN_4O$ m/z = 414.1247.

2-(6-Chloro-9H-carbazol-2-yl)-N'-(4-hydroxy-3-methoxybenzylidene)propanehydrazide (**14e**): white solid; yield: 90%; m. p. 239°C; ^{1}H NMR (600 MHz, DMSO-d_6, 25°C) δ = 11.37 and 11.30 (s, 1H), 11.36 and 11.12 (s, 1H), 9.49 and 9.45 (s, 1H), 8.17—6.78 (m, 10H), 4.78 and 3.82 (q, J = 7.0 Hz, 1H), 3.86 and 3.79 (s, 3H), 1.48 and 1.45 (d, J = 7.0 Hz, 3H) ppm; ^{13}C NMR (151 MHz, DMSO-d_6, 25°C) δ = 175.23 and 170.00, 149.32 and 148.95, 148.43, 147.54 and 143.19, 141.47 and 140.74, 141.07 and 141.03, 138.80 and 138.73, 126.27 and 126.12, 125.52 and 125.43, 124.13 and 124.09, 123.30 and 123.25, 122.41 and 121.65, 120.99, 120.84 and 120.61, 120.11 and 120.03, 119.71 and 119.25, 115.87 and 115.83, 112.80 and 112.72, 110.05 and 110.03, 109.35 and 109.27, 56.00 and 55.97, 44.87 and 41.85, 19.58 and 19.42 ppm; MS (ESI) m/z 422.13 = [M + H]$^+$, HRMS m/z 422.1266 = [M + H]$^+$, calcd. for $C_{23}H_{20}ClN_3O_3$ m/z = 421.1193.

2-(6-Chloro-9H-carbazol-2-yl)-N'-(4-chlorobenzylidene)propanehydrazide (**14f**): white solid; yield: 85%; m. p. 218°C; ^{1}H NMR (600 MHz, DMSO-d_6, 25°C) δ = 11.61 and 11.35 (s, 1H), 11.37 and 11.32 (s, 1H), 8.19 and 7.89 (s, 1H), 8.16 and 8.13 (d, J = 2.1 Hz, 1H), 8.09 and 8.05 (d, J = 8.1 Hz, 1H), 7.71 and 7.68 (s, 1H), 7.70 and 7.67 (s, 1H), 7.51—7.44 (m, 4H), 7.37—7.33 (m, 1H), 7.20—7.18 (m, 1H), 4.82 and 3.86 (q, J = 7.0 Hz, 1H), 1.48 (d, J = 7.0 Hz, 3H) ppm; ^{13}C NMR (151 MHz, DMSO-d_6, 25°C) δ = 175.64 and 170.44, 145.71, 141.70, 141.03, 140.94 and 140.48, 138.81 and 138.73, 134.82 and 134.52, 133.77 and 133.71, 129.37 and 129.33, 129.06 and 128.81, 125.55 and 125.47, 124.08, 123.31 and 123.26, 121.05 and 121.01, 120.91 and 120.68, 120.13 and 120.05, 119.54 and 119.25, 112.81 and 112.76, 110.32 and 110.10, 44.93, 41.63, 19.38 and 19.35 ppm; MS (ESI) m/z 410.15 = [M + H]$^+$, HRMS m/z 410.0798 = [M + H]$^+$, calcd. for $C_{22}H_{17}ClN_3O$ m/z = 409.0749.

2-(6-Chloro-9H-carbazol-2-yl)-N'-(2,4-dichlorobenzylidene)propanehydrazide (**14g**): white solid; yield: 82%; m. p. 241°C; ^{1}H NMR (600 MHz, DMSO-d_6, 25°C) δ = 11.83 and 11.53 (s, 1H), 11.38 and 11.32 (s, 1H), 8.54 and 8.24 (s, 1H), 8.17 and 8.13 (d, J = 2.1 Hz, 1H),

8.10 and 8.06 (d, J = 8.1 Hz, 1H), 8.02 and 7.91 (d, J = 8.5 Hz, 1H), 7.69 and 7.67 (d, J = 2.1 Hz, 1H), 7.54—7.45 (m, 3H), 7.37—7.33 (m, 1H), 7.19 and 7.18 (d, J = 1.5 Hz, 1H), 4.81 and 3.85 (q, J = 7.0 Hz, 1H), 1.48 (d, J = 7.0 Hz, 3H) ppm; ^{13}C NMR (151 MHz, DMSO-d_6, 25°C) δ = 175.76 and 170.56, 141.80 and 141.03, 140.83 and 140.29, 138.82 and 138.74, 137.98, 135.42 and 135.12, 134.16 and 133.96, 131.14 and 131.07, 129.81 and 129.79, 128.47, 128.43 and 128.30, 125.58 and 125.50, 124.06, 123.33 and 123.28, 121.12 and 121.07, 120.96 and 120.71, 120.14 and 120.06, 119.49 and 119.21, 112.83 and 112.78, 110.30 and 110.13, 45.11 and 41.73, 19.38 and 19.36 ppm; MS (ESI) m/z 443.92 = [M + H]$^+$, HRMS m/z 444.0430 = [M + H]$^+$, calcd. for $C_{22}H_{16}Cl_3N_3O$ m/z = 443.0359.

4.7 Crystal structure determination of **14a**

Crystal Data for $C_{23}H_{20}ClN_3O_3$ (M = 421.87 g/mol): triclinic, space group P-1 (no. 2), a = 10.7893 (14) Å, b = 13.0199 (15) Å, c = 15.497 (2) Å, α = 111.749 (12)°, β = 100.232 (11)°, γ = 90.146 (10)°, V = 1984.2 (5) Å^3, Z = 4, T = 149.99 (10) K, μ(Cu Kα) = 1.966 mm^{-1}, Dcalc = 1.412 g/cm^3, 13,393 reflections measured (7.33° ≤ 2Θ ≤ 148.834°), 7661 unique (R_{int} = 0.1060, R_{sigma} = 0.1452) which were used in all calculations. The final R_1 was 0.1024 (I > 2σ(I)) and wR_2 was 0.2727 (all data).

4.8 *In vitro* cytotoxicity assays

The *in vitro* cytotoxicity of these carbazole derivatives against human melanoma (A875), human gastric adenocarcinoma cells (7901), and a subclone of African green monkey kidney cell line MA-104 (MARC145) cell lines was evaluated using the MTT assay. Briefly, A875, 7901, and MARC145 cells were seeded at 2×10^4 cells per well in 96-well plates and grown to subconfluence. After removal of the growth medium, six serial dilutions of each tested compound in 200 μL test medium were added. Plates were incubated at 37°C in a humidified atmosphere containing 5% CO_2. After 72 h of exposure, the culture medium was removed and 30 μL of the MTT solution (5 mg/mL in PBS) was added to each well. The plate was further incubated for 4 h to allow MTT formazan formation. To dissolve the resulting MTT formazan, 50 μL of DMSO was added to each well, followed by thorough mixing with a microplate shaker. Absorbance at 570 nm was measured on a microplate reader (Thermo Scientific, MK3). All data were analyzed with SPSS software, and the 50% inhibitory concentrations (IC_{50}) of each compound for the different cell lines were determined. All assays were performed in triplicate on three independent experiments.

Data availability statement

The original contributions presented in the study are included in the article/Supplementary Material, further inquiries can be directed to the corresponding authors.

Author contributions

Conceptualization, XC and SK; methodology, ZG; validation, YC, YN, and KC; formal analysis, ZG and XC; writing—original draft preparation, ZG; writing—review and editing, XC and SK; funding acquisition, XC All authors have read and agreed to the published version of the manuscript.

Funding

Conflict of interest

The authors declare that the research was conducted in the absence of any commercial or financial relationships that could be construed as a potential conflict of interest.

Publisher's note

All claims expressed in this article are solely those of the authors and do not necessarily represent those of their affiliated organizations, or those of the publisher, the editors and the reviewers. Any product that may be evaluated in this article, or claim that may be made by its manufacturer, is not guaranteed or endorsed by the publisher.

Supplementary material

The Supplementary Material for this article can be found online at: https://www.frontiersin.org/articles/10.3389/fchem.2023.1104868/full#supplementary-material

References

Aggarwal, T. S., and Verma, A. K. (2019). Recent advances in the synthesis of carbazoles from indoles. *Org. Biomol. Chem.* 17 (36), 8330–8342. doi:10.1039/c9ob01381d

Bailly, C. (2020). Anticancer properties and mechanism of action of the quassinoid ailanthone. *Phytother. Res.* 34 (9), 2203–2213. doi:10.1002/ptr.6681

Bhutani, P., Joshi, G., Raja, N., Bachhav, N., Rajanna, P. K., Bhutani, H., et al.U.S. (2021). U.S. FDA approved drugs from 2015–june 2020: A perspective. *J. Med. Chem.* 64 (5), 2339–2381. doi:10.1021/acs.jmedchem.0c01786

Cao, S.-Y., Li, Y., Meng, X., Zhao, C.-N., Li, S., Gan, R.-Y., et al. (2019). Dietary natural products and lung cancer: Effects and mechanisms of action. *J. Funct. Foods* 52, 316–331. doi:10.1016/j.jff.2018.11.004

Caron, G., Digiesi, V., Solaro, S., and Ermondi, G. (2020). Flexibility in early drug discovery: Focus on the beyond-Rule-of-5 chemical space. *Drug Discov. Today* 25 (4), 621–627. doi:10.1016/j.drudis.2020.01.012

Chen, Y., Tang, C., Wu, Y., Mo, S., Wang, S., Yang, G., et al. (2015). Glycosmisines A and B: Isolation of two new carbazole–indole-type dimeric alkaloids from glycosmis pentaphylla and an evaluation of their antiproliferative activities. *Org. Biomol. Chem.* 13 (24), 6773–6781. doi:10.1039/c5ob00695c

Dang, Z., Xu, S., Zhang, H., Gui, W., Zhao, Y., Duan, L., et al. (2018). *In vitro* and *in vivo* efficacies of carbazole aminoalcohols in the treatment of alveolar echinococcosis. *Acta Trop.* 185, 138–143. doi:10.1016/j.actatropica.2018.05.007

Davison, E. K., and Sperry, J. (2017). Natural products with heteroatom-rich ring systems. *J. Nat. Prod.* 80 (11), 3060–3079. doi:10.1021/acs.jnatprod.7b00575

Duangdee, N., Mahavorasirikul, W., and Prateeptongkum, S. (2020). Design synthesis and anti-proliferative activity of some new coumarin substituted hydrazide–hydrazone derivatives. *J. Chem. Sci.* 132 (1), 66–12. doi:10.1007/s12039-020-01767-4

Fang, Y., Li, H., Ji, B., Cheng, K., Wu, B., Li, Z., et al. (2021). Renieramycin-type alkaloids from marine-derived organisms: Synthetic chemistry, biological activity and structural modification. *Eur. J. Med. Chem.* 210, 113092. doi:10.1016/j.ejmech.2020.113092

Favia, A. D., Habrant, D., Scarpelli, R., Migliore, M., Albani, C., Bertozzi, S. M., et al. (2012). Identification and characterization of carprofen as a multitarget fatty acid amide hydrolase/cyclooxygenase inhibitor. *J. Med. Chem.* 55 (20), 8807–8826. doi:10.1021/jm3011146

Greco, G., Catanzaro, E., and Fimognari, C. (2021). Natural products as inducers of non-canonical cell death: A weapon against cancer. *Cancers (Basel)* 13 (2), 304. doi:10.3390/cancers13020304

Gu, Y., Huang, W., Chen, S., and Wang, X. (2018). Bismuth(III) triflate catalyzed three-component reactions of indoles, ketones, and alpha-bromoacetaldehyde acetals enable indole-to-carbazole transformation. *Org. Lett.* 20 (14), 4285–4289. doi:10.1021/acs.orglett.8b01707

Han, Y., Tian, Y., Wang, R., Fu, S., Jiang, J., Dong, J., et al. (2020). Design, synthesis and biological evaluation of thieno[3, 2-d]pyrimidine derivatives containing aroyl hydrazone or aryl hydrazide moieties for PI3K and mTOR dual inhibition. *Bioorg Chem.* 104, 104197. doi:10.1016/j.bioorg.2020.104197

Huang, W., Gao, Z., Zhang, Z., Fang, W., Wang, Z., Wan, Z., et al. (2021). Selective and effective anticancer agents: Synthesis, biological evaluation and structure-activity relationships of novel carbazole derivatives. *Bioorg Chem.* 113, 104991. doi:10.1016/j.bioorg.2021.104991

Issa, S., Prandina, A., Bedel, N., Rongved, P., Yous, S., Le Borgne, M., et al. (2019). Carbazole scaffolds in cancer therapy: A review from 2012 to 2018. *J. Enzyme Inhib. Med. Chem.* 34 (1), 1321–1346. doi:10.1080/14756366.2019.1640692

Kong, X., Zhang, H., Cao, C., Zhou, S., Pang, G., and Shi, Y. (2016). Synthesis of fluorinated carbazoles via C-H arylation catalyzed by Pd/Cu bimetal system and their antibacterial activities. *Bioorg Med. Chem.* 24 (6), 1376–1383. doi:10.1016/j.bmc.2016.02.013

Liu, L. X., Wang, X. Q., Zhou, B., Yang, L. J., Li, Y., Zhang, H. B., et al. (2015). Synthesis and antitumor activity of novel N-substituted carbazole imidazolium salt derivatives. *Sci. Rep.* 5, 13101. doi:10.1038/srep13101

Liu, Y. P., Hu, S., Liu, Y. Y., Zhang, M. M., Zhang, W. H., Qiang, L., et al. (2019). Anti-inflammatory and antiproliferative prenylated carbazole alkaloids from Clausena vestita. *Bioorg Chem.* 91, 103107. doi:10.1016/j.bioorg.2019.103107

Liu, Y. P., Li, Y. J., Zhao, Y. Y., Guo, J. M., Liu, Y. Y., Wang, X. P., et al. (2021). Carbazole alkaloids from the fruits of Clausena anisum-olens with potential PTP1B and alpha-glucosidase inhibitory activities. *Bioorg Chem.* 110, 104775. doi:10.1016/j.bioorg.2021.104775

Liu, Y., Wu, Y., Sun, L., Gu, Y., and Hu, L. (2020). Synthesis and structure-activity relationship study of water-soluble carbazole sulfonamide derivatives as new anticancer agents. *Eur. J. Med. Chem.* 191, 112181. doi:10.1016/j.ejmech.2020.112181

Mellini, P., Carafa, V., Di Rienzo, B., Rotili, D., De Vita, D., Cirilli, R., et al. (2012). Carprofen analogues as sirtuin inhibitors: Enzyme and cellular studies. *ChemMedChem* 7 (11), 1905–1908. doi:10.1002/cmdc.201200318

Murali, K., Sparkes, H. A., and Rajendra Prasad, K. J. (2017). Synthesis of hetero annulated isoxazolo-pyrido- and pyrimido carbazoles: Screened for *in vitro* antitumor activity and structure activity relationships, a novel 2-amino-4-(3'-bromo-4'-methoxyphenyl)-8-chloro-11H-pyrimido[4, 5-a]carbazole as an antitumor agent. *Eur. J. Med. Chem.* 128, 319–331. doi:10.1016/j.ejmech.2017.02.009

Newman, D. J., and Cragg, G. M. (2020). Natural products as sources of new drugs over the nearly four decades from 01/1981 to 09/2019. *J. Nat. Prod.* 83 (3), 770–803. doi:10.1021/acs.jnatprod.9b01285

Padmaja, P., Koteswara Rao, G., Indrasena, A., Subba Reddy, B. V., Patel, N., Shaik, A. B., et al. (2015). Synthesis and biological evaluation of novel pyrano[3, 2-c]carbazole derivatives as anti-tumor agents inducing apoptosis via tubulin polymerization inhibition. *Org. Biomol. Chem.* 13 (5), 1404–1414. doi:10.1039/c4ob02015d

Peng, S., Wang, Y., Zhou, Y., Ma, T., Wang, Y., Li, J., et al. (2019). Rare ginsenosides ameliorate lipid overload-induced myocardial insulin resistance via modulating metabolic flexibility. *Phytomedicine* 58, 152745. doi:10.1016/j.phymed.2018.11.006

Peng, X., Sun, Z., Kuang, P., Li, L., Chen, J., and Chen, J. (2020). Copper-catalyzed selective arylation of nitriles with cyclic diaryl iodonium salts: Direct access to structurally diversified diarylmethane amides with potential neuroprotective and anticancer activities. *Org. Lett.* 22 (15), 5789–5795. doi:10.1021/acs.orglett.0c01829

Percy, S., Mancand, D. L. C., Belica, P. S., Wong, F., Harry, S., and Wnng, L. B. (1994). Syntheses of carprofen, a carbazole-based nonsteroidal anti-inflammatory agent. *Heterocycles* 39 (2), 833–845. doi:10.3987/com-94-s(b)83

Popiolek, L., Piatkowska-Chmiel, I., Gawronska-Grzywacz, M., Biernasiuk, A., Izdebska, M., Herbet, M., et al. (2018). New hydrazide-hydrazones and 1, 3-thiazolidin-4-ones with 3-hydroxy-2-naphthoic moiety: Synthesis, *in vitro* and *in vivo* studies. *Biomed. Pharmacother.* 103, 1337–1347. doi:10.1016/j.biopha.2018.04.163

Rassias, G., Zogali, V., Swarbrick, C. M. D., Ki Chan, K. W., Chan, S. A., Gwee, C. P., et al. (2019). Cell-active carbazole derivatives as inhibitors of the zika virus protease. *Eur. J. Med. Chem.* 180, 536–545. doi:10.1016/j.ejmech.2019.07.007

Sun, L., Wang, C., Hu, X., Wu, Y., Jiang, Z., Li, Z., et al. (2020). Design, synthesis, and evaluations of the antiproliferative activity and aqueous solubility of novel carbazole sulfonamide derivatives as antitumor agents. *Bioorg Chem.* 99, 103766. doi:10.1016/j.bioorg.2020.103766

Sun, L., Wu, Y., Liu, Y., Chen, X., and Hu, L. (2017). Novel carbazole sulfonamide derivatives of antitumor agent: Synthesis, antiproliferative activity and aqueous solubility. *Bioorg Med. Chem. Lett.* 27 (2), 261–265. doi:10.1016/j.bmcl.2016.11.068

Sung, H., Ferlay, J., Siegel, R. L., Laversanne, M., Soerjomataram, I., Jemal, A., et al. (2021). Global cancer statistics 2020: GLOBOCAN estimates of incidence and mortality worldwide for 36 cancers in 185 countries. *CA Cancer J. Clin.* 71 (3), 209–249. doi:10.3322/caac.21660

Thomas, S. M., Purmal, A., Pollastri, M., and Mensa-Wilmot, K. (2016). Discovery of a carbazole-derived lead drug for human african trypanosomiasis. *Sci. Rep.* 6, 32083. doi:10.1038/srep32083

Wang, G., Sun, S., and Guo, H. (2022). Current status of carbazole hybrids as anticancer agents. *Eur. J. Med. Chem.* 229, 113999. doi:10.1016/j.ejmech.2021.113999

Wang, W., Li, Q., Wei, Y., Xue, J., Sun, X., Yu, Y., et al. (2017). Novel carbazole aminoalcohols as inhibitors of beta-hematin formation: Antiplasmodial and antischistosomal activities. *Int. J. Parasitol. Drugs Drug Resist* 7 (2), 191–199. doi:10.1016/j.ijpddr.2017.03.007

Wang, Y., Yao, H., Hua, M., Jiao, Y., He, H., Liu, M., et al. (2020). Direct N-glycosylation of amides/amines with glycal donors. *J. Org. Chem.* 85 (11), 7485–7493. doi:10.1021/acs.joc.0c00975

Wu, X. T., Xiao, E. K., Ma, F., Yin, J., Wang, J., Chen, P., et al. (2021). Substrate-controlled regiodivergent synthesis of fluoroacylated carbazoles via Friedel-Crafts acylation. *J. Org. Chem.* 86 (9), 6734–6743. doi:10.1021/acs.joc.1c00473

Xie, J., Xu, W., Song, H., Liu, Y., Zhang, J., and Wang, Q. (2020). Synthesis and antiviral/fungicidal/insecticidal activities study of novel chiral indole diketopiperazine derivatives containing acylhydrazone moiety. *J. Agric. Food Chem.* 68 (20), 5555–5571. doi:10.1021/acs.jafc.0c00875

Xie, Z., Wei, Y., Xu, J., Lei, J., and Yu, J. (2019). Alkaloids from piper nigrum synergistically enhanced the effect of paclitaxel against paclitaxel-resistant cervical cancer cells through the downregulation of Mcl-1. *J. Agric. Food Chem.* 67 (18), 5159–5168. doi:10.1021/acs.jafc.9b01320

Yang, Y., Liu, Q., Shi, X., Zheng, Q., Chen, L., and Sun, Y. (2021). Advances in plant-derived natural products for antitumor immunotherapy. *Arch. Pharm. Res.* 44 (11), 987–1011. doi:10.1007/s12272-021-01355-1

Yokoyama, T., Yukuhiro, M., Iwasaki, Y., Tanaka, C., Sankoda, K., Fujiwara, R., et al. (2019). Identification of candidate molecular targets of the novel antineoplastic antimitotic NP-10. *Sci. Rep.* 9 (1), 16825. doi:10.1038/s41598-019-53259-2

Zhou, Y., Li, C., Peng, J., Xie, L., Meng, L., Li, Q., et al. (2018). DNA-Encoded dynamic chemical library and its applications in ligand discovery. *J. Am. Chem. Soc.* 140 (46), 15859–15867. doi:10.1021/jacs.8b09277